Applied Catalysis B: Environmental 237 (2018) 673–680

Contents lists available at ScienceDirect

Applied Catalysis B: Environmental

journal homepage: www.elsevier.com/locate/apcatb

Enhanced CO_2 reduction activity of polyethylene glycol-modified Au nanoparticles prepared via liquid medium sputtering

Min Wook Chung[a,1], In Young Cha[a,1], Min Gwan Ha[a], Youngseung Na[a], Jungsoo Hwang[a], Hyung Chul Ham[a,b], Hyoung-Juhn Kim[a,b], Dirk Henkensmeier[a,b,c], Sung Jong Yoo[a,b,c], Jin Young Kim[a,b,c], So Young Lee[a], Hyun S. Park[a,*], Jong Hyun Jang[a,b,c,**]

[a] Fuel Cell Research Center, Korea Institute of Science and Technology (KIST), Seoul 02792, Republic of Korea
[b] Division of Energy & Environment Technology, KIST School, University of Science and Technology (UST), Seoul 02792, Republic of Korea
[c] Green School, Korea University, Seoul 02841, Republic of Korea

ARTICLE INFO

Keywords:
Electrochemistry
CO_2reduction
Electrocatalyst
Liquid medium sputtering
Gold nanoparticle

ABSTRACT

The electrochemical conversion of CO_2 into useful chemicals such as CO is a promising strategy to reduce CO_2 emissions from fossil fuel consumption and to mitigate the impacts of global warming. Although tremendous effort has been devoted to the practical use of CO_2conversion techniques, these techniques still suffer from deficient catalytic activity toward CO_2 reduction as well as a complex catalyst synthesis procedure. In this study, an effective strategy to enhance the catalytic CO_2 reduction activity with a unique synthesis method is proposed. Polyethylene glycol (PEG)-coated Au nanoparticles supported on a porous carbon support are prepared by a facile, cost-effective, and biocompatible one-step sputtering deposition method, termed liquid medium sputtering. The use of PEG as a liquid medium is advantageous in terms of catalytic activity and stability by producing PEG layers on the Au surface. The prepared PEG-coated Au nanoparticle catalyst exhibits a CO Faradaic efficiency of 100% at $-0.57\ V_{RHE}$ and excellent stability during 10 h of operation due to the high solubility of PEG for CO_2.

1. Introduction

The increasing concentration of atmospheric carbon dioxide (CO_2) causes various environmental and economic issues, as epitomized by global warming and climate changes [1]. In order to reduce the impacts of global warming, there have been many efforts to reduce CO_2 emission and the concentration of atmospheric CO_2 by employing techniques like sequestration, chemical hydrogenation, and electrochemical reduction of CO_2 [2,3]. CO_2 conversion into value-added fuels is an environmentally and industrially efficient method to address the greenhouse gas problem. As an established CO_2 conversion method, the approach comprising electrochemical reduction of CO_2 is an attractive method for sustainable energy storage and fuel production because it utilizes renewable electricity sources such as solar and wind power [4,5].

Using the electrochemical reduction system, CO_2 is transformed into various chemical products such as CO, HCOOH, CH_4, CH_3OH, and C_2H_4 [6–11]. Among such products, CO is a useful and invaluable feedstock because it can be used to readily produce an assortment of hydrocarbons via the Fischer–Tropsch process. Further, the production of CO by electrochemical reactions has great advantages in terms of product usage and cost-effectiveness; for instance, the gas mixture of CO and H_2, so-called 'syngas', can feasibly be generated in an electrochemical device to reduce CO_2 and H^+, where water oxidation occurs at the anode to give oxygen and electrons. The syngas composition is controlled by the electrochemical operating factors such as the cell voltage, electrolyte composition, and type of electrocatalyst [4,6,12]. For these reasons, electrochemical CO_2 reduction is quite attractive from an economical point of view because optimizing the conditions for the electrochemical production of syngas can eliminate the gas separation step [5].

However, because the electrochemical reduction of CO_2 involves the transfer of multiple electrons, resulting in sluggish kinetics, the success of this system requires the development of catalytic surfaces with good catalytic activity, selectivity, and stability. For the electrochemical production of CO from CO_2, Au is a representative catalyst; compared

* Corresponding author.
** Corresponding author at: Fuel Cell Research Center, Korea Institute of Science and Technology (KIST), Seoul 02792, Republic of Korea.
E-mail addresses: hspark@kist.re.kr (H.S. Park), jhjang@kist.re.kr (J.H. Jang).
[1] Authors contributed equally to this work.

https://doi.org/10.1016/j.apcatb.2018.06.022
Received 2 April 2018; Received in revised form 4 June 2018; Accepted 8 June 2018
Available online 09 June 2018
0926-3373/

with other metals such as Ag, Cu, Zn, Fe, or Pt, Au has an ideal CO binding energy at approximately −0.4 eV [12]. The binding energy between a metal-based catalyst and CO influences the catalytic performance in CO_2 conversion processes, and the stability of the *COOH reaction intermediate is strongly correlated with that of CO. Metals that bind CO strongly cause CO poisoning of the catalyst surfaces rather than CO production, leading to hydrogen evolution by way of proton reduction. However, metal surfaces that bind CO weakly have low activity for the CO_2 reduction reaction because of slower activation of CO_2 to *COOH, which is the first step in the CO_2 reaction sequence [13].

Density functional theory calculations have predicted the binding energy for CO on the Au surface to be ca. −0.4 eV, which is believed to be the ideal binding energy for CO_2 reduction [12]. Accordingly, tremendous effort has been devoted to manipulating the Au surface for CO_2 reduction by fabricating nano-structured materials, introducing strong support–catalyst interactions, and alloying Au with other metals [14–16]. Of these approaches, the utilization of nano-structured Au has received much attention because it demonstrates an increased number of active edge sites; it has been experimentally and theoretically reported that edge sites have a higher ability to reduce CO_2 than basal planes [17,18]. Additionally, the mass-normalized catalytic activity and material utilizations should also be enhanced as the number of active sites increase in the electrochemical reactions.

Many studies on nano-structured Au have reported various synthetic methods including galvanic displacement [14], chemico-thermal reduction using organic ligands [16,18], electrodeposition [19], and ionic liquid sputtering [20,23–25]. Plus, different synthetic techniques have been developed to produce highly active nanostructures through simple and facile procedures for catalytic reductions. Among them, liquid medium sputtering has recently attracted considerable attention [20,23–25].

Liquid sputtering generates uniformly sized metal nanoparticles by the direct dispersion of metal precursors in an ionic liquid and organic solvents [20,23]. The physical vapor technique can convert the bulk metals into smaller nanoparticles in a few simple steps without complex reduction or ligand chemistry, making it a suitable process for large-scale catalyst production. Moreover, this technique makes use of well-developed vacuum sputtering equipment by dispersing the deposited catalyst and/or catalyst supports in a liquid substrate, such as an ionic liquid or non-volatile polymer with extremely low vapor pressure, instead of the typical solid-phase substrate. Ejected metal particles from the target material are dispersed in the liquid medium and sequentially form a colloidal solution that enables this technique to achieve uniformity and control of metal nanoparticles in terms of shape and composition, respectively. Furthermore, if support materials are dispersed in the liquid medium, metal nanoparticles deposited on the support material can be obtained easily without further processing [23].

Herein, we introduce carbon-supported Au nanoparticles through a straightforward, cost-effective, surfactant-free, and biocompatible one-step liquid medium sputtering method that has not yet been reported in the CO_2 electro-reduction field. Given the optimum CO binding energy at its surface and the advantages of the liquid sputtering technique, Au nanoparticles layered on a carbon support produced by liquid sputtering are suitable for practical CO_2 reduction applications for two primary reasons. Firstly, the synthetic process does not require an organic surfactant and its subsequent removal during the growth and collection processes, whereas colloidal nanoparticle synthesis often uses organic surfactants. Further, ligand chemistry in the colloidal synthesis is required to avoid nanoparticle agglomeration during particle formation. However, the surfactants are difficult to remove, even with harsh conditions such as acid treatment and/or calcination; consequently, the surfactant residues limit electrocatalytic reactions on the catalyst surface [20,21]. Secondly, the technique produces a well-dispersed catalyst on the conductive and high surface area carbon support. The use of bare nanoparticles as an electrocatalyst usually suffers from the densely packed structure, resulting in high transfer resistance of reactants and products within the catalyst layer [22]. Thus, catalysts dispersed on a high surface area support with a surfactant-free synthesis procedure should be utilized as an electrocatalysts for CO_2 reduction. In this study, polyethylene glycol (PEG) is selected as a liquid substrate with the expectation that the PEG layer will be automatically deposited onto the carbon-supported Au nanoparticles during the synthesis. Thus, the PEG layer will benefit both the reduction of CO_2 and the stability of the prepared catalyst due to its intrinsically high CO_2 solubility.

2. Experimental

2.1. Catalyst synthesis

RF sputter deposition was performed with a KVS-2004 sputtering system at a base pressure of 1×10^{-5} Torr and an Ar working pressure of 1×10^{-2} Torr. Pure Au (99.95%) targets were located 20 cm away from the liquid substrate. PEG with an average molecular weight of 600 g was purchased from Sigma-Aldrich and used without further purification. In order to form supported Au nanoparticle catalysts, carbon powder (20 mg, Vulcan XC-72) was dispersed in 20 mL PEG 600, and the carbon-containing solvent was transferred to the sputtering chamber. Carbon-supported gold nanoparticles (Au/C) were prepared by Au sputtering with a power of 300 W for 1 h. After Au sputtering onto the liquid medium was completed, vacuum annealing within the sputtering chamber was further conducted to strengthen the binding forces between the Au nanoparticles and the carbon supports. The resulting Au/C was filtered and purified using cuprous ethanol solvent. After filtering with ethanol, the samples (LS-PEG) were dried at 75 °C for 5 h. For the PEG-removed Au/C sample (LS), heat-treatment under an Ar atmosphere at 400 °C was conducted for 2 h to remove the PEG layers. As a reference, commercial Au/C catalyst (CM) was purchased from Premetek. PEG-coated commercial Au/C (CM-PEG) was also prepared by overnight stirring of a solution containing CM and PEG 600 with sequential filtering and drying.

2.2. Physical characterization

The morphology and structure of the prepared catalysts were analyzed by transmission electron microscopy (TITAN™ 80–300, FEI). Thermogravimetric analysis (Q50 TGA, TA Instruments) was conducted within the temperature range from 24 to 900 °C at a heating rate of 10 °C/min under atmospheric conditions. X-ray diffraction (XRD, Dmax2500/PC, RIGAKU) was performed to determine the crystal structure of the prepared catalysts. X-ray photoelectron spectroscopy (PHI 5000 VersaProbe, Ulvac-PHI) and X-ray absorption near edge structure (XANES, RIGAKU) were conducted to identify the electronic structure of the prepared catalysts.

2.3. Electrochemical characterization

The catalytic activity of the prepared catalysts toward CO_2 reduction was measured by a conventional three electrode system. The working electrode was prepared by drop-casting 0.02 mL of catalyst ink onto a glassy carbon (GC) electrode with a 5 mm diameter. The catalyst ink contained 5 mg of the catalyst, 25 μL of Nafion solution (5 wt.% in lower aliphatic alcohols and 15–20% water, Sigma-Aldrich), and 0.75 mL of isopropyl alcohol. The Ag/AgCl electrode and Pt mesh were used as the reference and counter electrodes, respectively. All potentials described in this work were referenced to the reversible hydrogen electrode (RHE). The electrolyte for the electrochemical measurements was either a CO_2- or Ar-saturated 0.5 M $KHCO_3$ (99.7%, Sigma-Aldrich) aqueous solution. Linear sweep voltammetry (LSV) and chronoamperometry (CA) were performed using a PGSTAT30 potentiostat (Autolab). During the experiments, the product of the CO_2 reduction

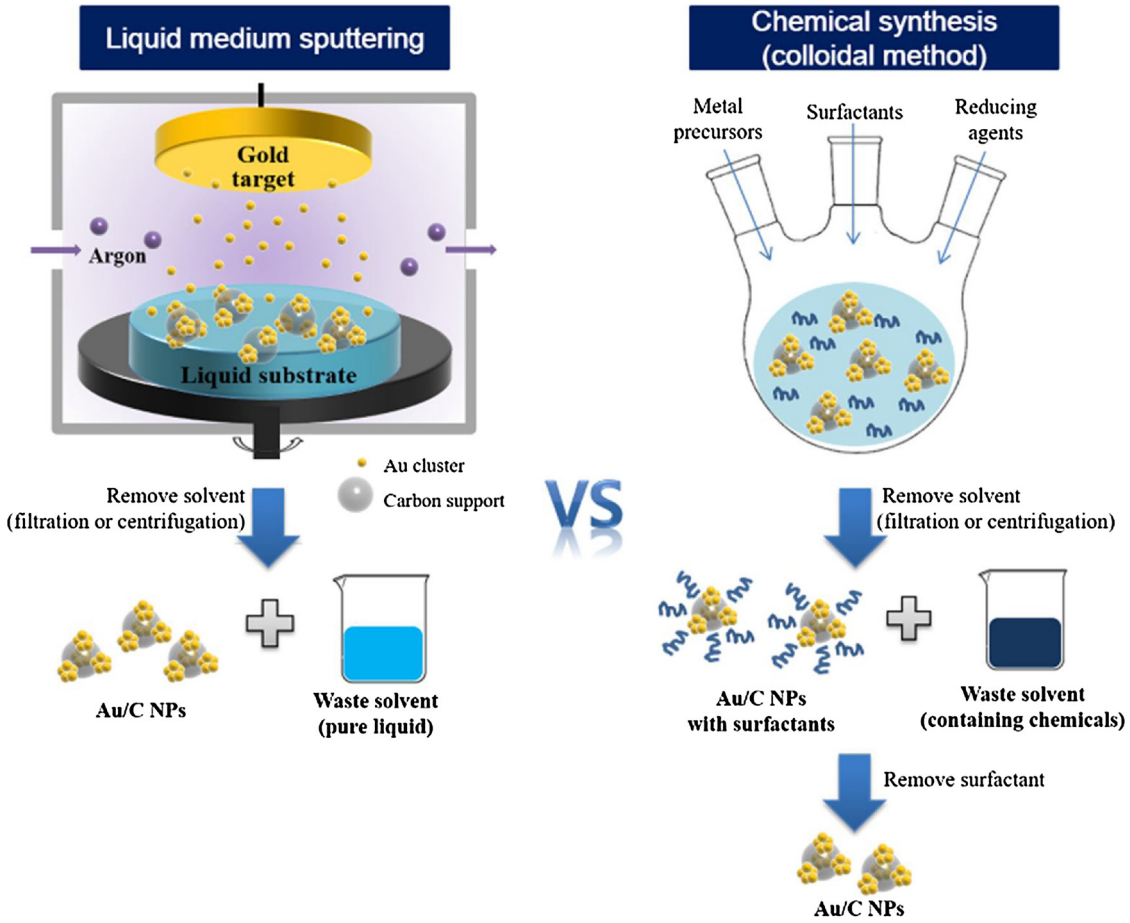

Fig. 1. Scheme of liquid medium sputtering method and chemical synthesis method (representatively colloidal method).

reactions was analyzed using gas chromatography (GC, 7890B, Agilent Inc.).

3. Results and discussion

3.1. Catalyst preparation

The PEG-coated Au/C catalyst (LS-PEG) was prepared via a liquid medium sputtering method. Collision between inert gas molecules and the Au target generated Au nanoparticles, which were deposited directly on Vulcan carbon in the liquid medium (i.e., PEG 600). It should be noted that the use of the liquid medium sputtering method enables the one-step synthesis of Au/C catalysts, unlike typical chemical reduction syntheses, such as the colloidal method compared schematically in Fig. 1. As discussed above, the facile and simple preparation of Au/C from the liquid sputtering method is economically and environmentally efficient given that its catalytic performance for CO_2 reduction is ensured.

The size of the sputtered Au nanoparticles on Vulcan carbon was studied in SEM (Fig. 2). The size of the Au prepared in the LS-PEG ranged from a few nanometers to tens of nanometers, and their average value was 11 nm, as confirmed by particle size distribution analysis (Fig. 2a and b). Non-volatile ionic liquids with a high boiling point and low vapor pressure, for example, 1-ethyl-3-methylimidazolium tetrafluoroborate, 1-butyl-3-methylimidazolium hexafluorophosphate, or N,N,N-trimethyl-N-propylammonium bis-(trifluoromethanesulfonyl) imide, are commonly used as the liquid medium in sputtering techniques [24–31]. Given that liquid sputtering using non-volatile long-chain liquid chemicals results in particle sizes in the range of a few nanometers [24–31], the slightly large particle size obtained in this study may originate from the different physicochemical properties of PEG 600 relative to ionic liquids, as well as the interaction between Au and the medium. For example, Pt nanoparticles with an approximate size of 2 nm were fabricated by liquid sputtering in PEG 600 [23]. Investigations on seeding and the growth mechanism of sputtered Au in PEG 600 are currently in progress in our laboratory to gain greater control of the Au nanoparticle size.

In this study, heat treatment was only performed when removal of the PEG coating on Au/C was desired (Fig. 2c and d) or for any additional synthetic procedure, which is typically required to remove the organic surfactants and was intentionally omitted before the catalyst investigations. When heat treatment was necessary, PEG-removed Au/C catalyst (LS) was formed by an additional thermal process at 400 °C under an Ar atmosphere for 2 h. Following heat treatment, the average particle size of LS was slightly increased to approximately 14 nm owing to inevitable agglomeration of nanoparticles at high temperature (Fig. 2c and d). The PEG layers on the Au/C nanoparticle surface were likely exfoliated by thermal annealing, as discussed below.

Otherwise, the PEG layer deposited onto the Au/C catalyst was intentionally preserved in the synthesis as the PEG coating could benefit the CO_2 reduction performance. In the electrochemical CO_2 reduction in aqueous electrolyte solutions, the mass transport of CO_2 to the electrode surfaces is considered as an important factor in determining the reduction selectivity and activity [5,32]. Higher surface concentrations of CO_2 at the electrode increase the exchange current density and shift the thermodynamic standard potential to positive values for CO_2 reduction [33]. Note that the CO_2 solubility of PEG is 5.8 times higher than that of water (i.e. 8.7 g L^{-1} for PEG 600 and 1.5 g L^{-1} for water) [34].

The presence of the PEG layer on the Au/C catalysts was confirmed

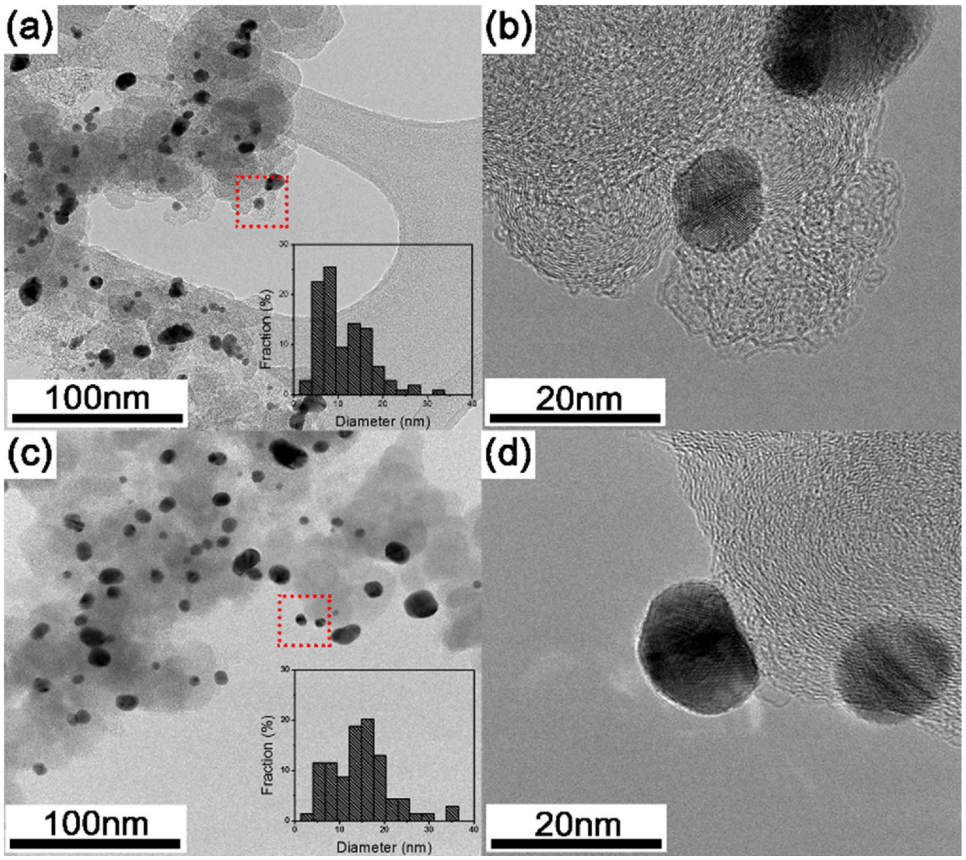

Fig. 2. Representative TEM images of (a) LS-PEG, (b) magnified TEM images of LS-PEG, (c) TEM images of LS and (d) magnified TEM images of LS. (a inset) and (c inset) are particle size distribution of LS-PEG and LS based on the TEM images, respectively.

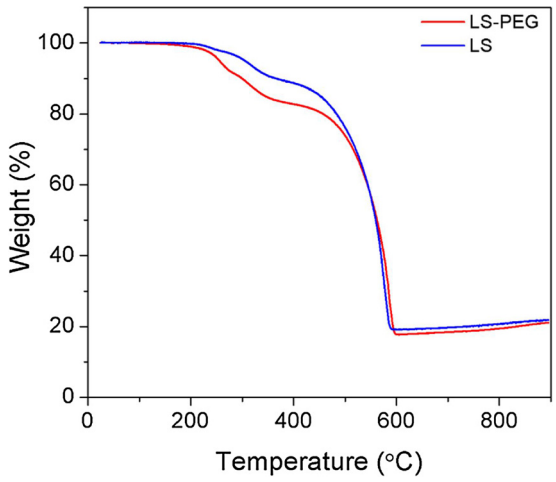

Fig. 3. TGA measurements of LS-PEG (red) and LS (blue).

by TGA analysis (Fig. 3). The mass loss of LS-PEG and LS as the temperature increased was measured in the temperature range from 24 to 900 °C at a heating rate of 10 °C/min under atmospheric conditions. The mass decrease displayed at temperatures higher than 100 °C was more distinct for LS-PEG than LS, and a larger mass decrease for LS-PEG than LS was observed at temperatures between 250 and 400 °C (Fig. 3). The temperature corresponding to the larger mass loss of LS-PEG coincides with the flash point of PEG 600 (i.e., 273 °C). The TGA results indicate that more PEG was present on LS-PEG; similar TGA behavior of PEG-containing materials was reported previously for a Pt/PEG composite film [35]. At temperatures above 600 °C, the remaining mass percent of LS-PEG and LS is approximately identical, indicating that both catalysts contain a similar Au content on the carbon support (i.e., *ca.* 20 wt.%). Based on the calculated mass percent remaining at 400 °C, where no further mass loss by PEG is expected, the PEG content for LS-PEG and LS was estimated to be 17.33 and 11.39 wt.%, respectively, indicating that the surface PEG layers were partially removed by the heat treatment process.

Nevertheless, the heat treatment conducted to exfoliate the PEG layers did not affect the Au nanoparticle structure on the Vulcan carbon, as confirmed by XRD and XPS analyses (Figs. 4 and S1). In the XRD results of LS-PEG and LS (Fig. 4), characteristic peaks of face-

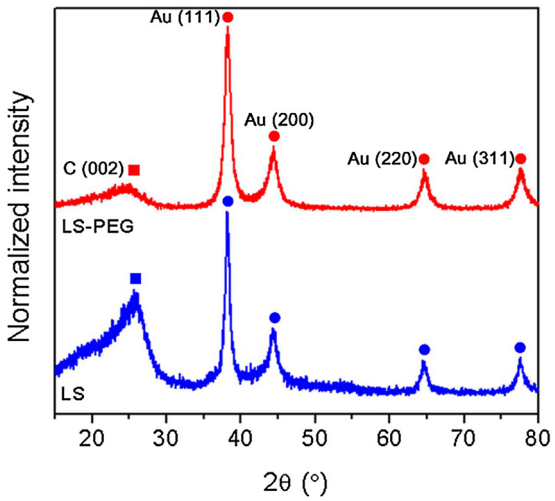

Fig. 4. XRD patterns of LS-PEG (red) and LS (blue). Solid square indicates the diffraction pattern of carbon, and solid circle for Au.

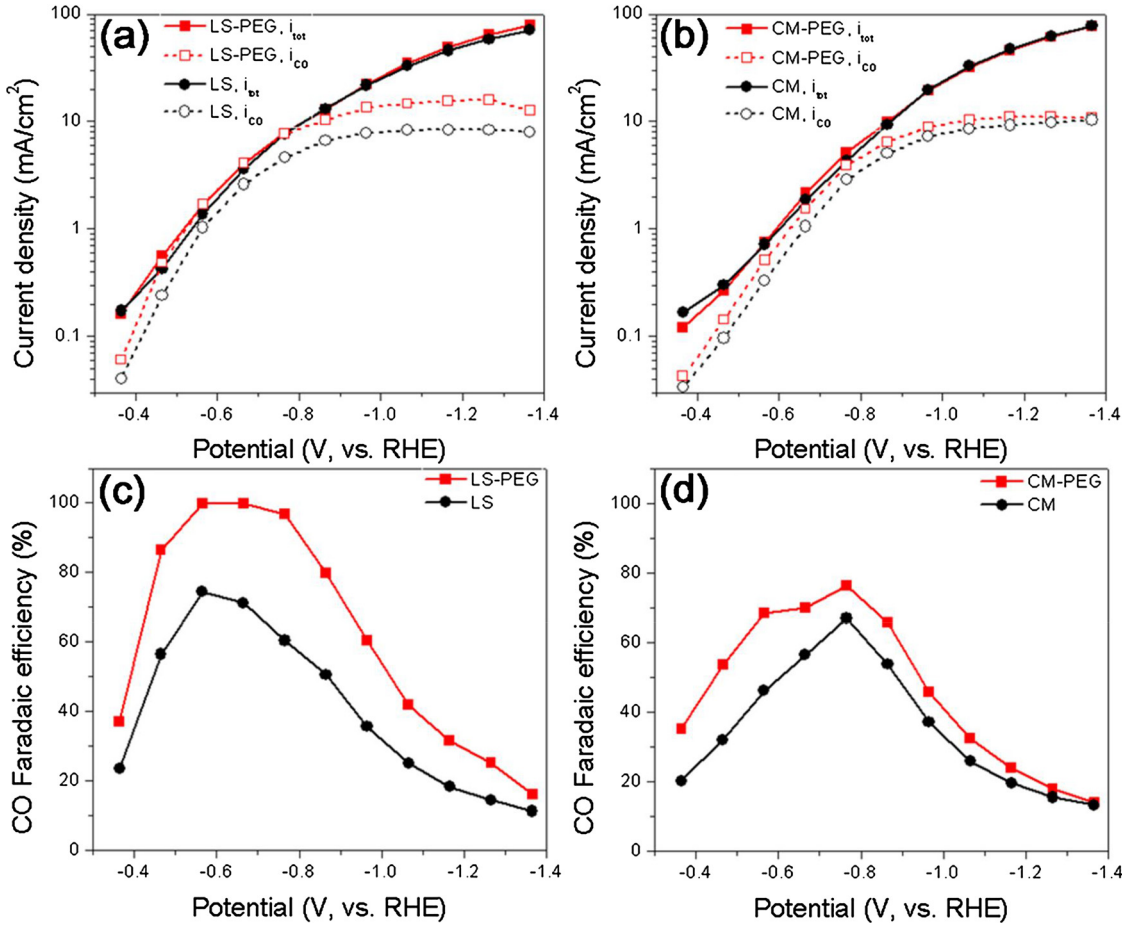

Fig. 5. Electrochemical CO_2 reduction activities of the prepared catalysts. Total current density and partial CO current density of (a) LS-PEG and LS, and (b) CM-PEG and CM. CO Faradaic efficiency of (c) LS-PEG and LS, and (d) CM-PEG and CM. Performances were measured by three electrode system with Pt mesh as counter electrode and Ag/AgCl as reference electrode. CO_2-saturated 0.5 M $KHCO_3$ solution was used as electrolyte.

centered cubic structure of Au were identically observed at 38°, 44.5°, 64.6°, and 77.6°, which correspond to the patterns of Au(111), (200), (220), and (311), respectively (JCPDS, #04-0784). However, a strengthened carbon (002) peak at 26° in LS was observed, possibly due to the exposed Vulcan carbon after removal of the PEG layers and the additional heat treatment.

3.2. Electrochemistry

The activities of the electrochemical CO_2 reduction of the prepared catalysts, including commercial Au/C, were examined by CA at different potentials ranging from −0.37 to −1.37 V in a CO_2-saturated 0.5 M $KHCO_3$ electrolyte. In order to analyze the final products and the activity and selectivity of the electrodes for CO_2 reduction, the gaseous products were analyzed by GC. The prepared Au catalysts of LS-PEG and LS exhibited a similar total reduction current in the LSV experiments (Fig. 5a, solid symbol and line) of approximately 10 mA/cm^2 at −0.8 V. However, the reaction selectivity and partial current density of LS-PEG toward CO production is significantly higher than that of LS across the entire range of potentials examined. The CO production partial current density of LS-PEG is larger than 10 mA/cm^2, and it is at least 3 mA/cm^2 higher than that of LS at potentials more negative than −0.9 V (Fig. 5a, empty symbol and dotted line). Accordingly, the reaction selectivity (i.e., faradaic efficiency) of LS-PEG for CO_2 reduction is higher than that of LS. For instance, the maximum CO faradaic efficiency of LS-PEG and LS at −0.57 V were 100 and 74.5%, respectively.

The significant difference in performance of LS-PEG and LS for CO_2 reduction can be explained in terms of two major factors: i) the presence of the PEG-layer on the Au/C surfaces in the catalyst preparation process, and ii) the slightly smaller Au particle size in LS-PEG than LS (i.e., approximately 11 and 14 nm, respectively). The particle size of Au catalysts has been reported to affect both the activity and selectivity of the electrochemical CO_2 reduction [36,37]. Given that surface area limits the electrochemical reaction rate, the total current density should increase as the particle size is decreased. To this end, the particle diameter in LS-PEG is 27% smaller than that in LS, implying that the total current density would be larger. Indeed, it is estimated to be almost 27% larger for LS-PEG if surface area were the only governing factor for the CO_2 reduction reaction. However, the CO_2 reduction reaction rate including proton reduction, that is, the two main reactions at the Au/C surface in a CO_2 saturated aqueous solution, is significantly dominated by the surface properties and reaction kinetics, as in other multi-electron transfer reactions. The total current densities of LS-PEG and LS are actually similar to each other, as shown in Fig. 5a, indicating that the reactions at LS-PEG and LS are not actually determined by surface area. The electrochemical CO_2 reduction is reported to be dependent on the properties of the surface exposed to the electrolyte [36,37]. As differently sized nanoparticles present a distinct number of unique facets to the electrolyte, the CO_2 reduction activity also depends on the nanoparticle size. For example, the CO formation rate was increased approximately 100 times as the particle size decreased from 5 nm to 25 Au atoms [36]. Similarly, the Faradaic current densities of the CO_2 reduction at −1.2 V were reduced from approximately 600 to less than 50 mA/cm$^2_{AU}$ as the particle size increased from 1 to 8 nm [37]. However, the sizes of both the Au nanoparticles prepared in this study are too large (i.e., 11 and 14 nm, close to the bulk crystals) to

affect the CO_2 reduction activity [36,37].

As discussed above, PEG has a CO_2 solubility that is 5.8 times higher than water (i.e., 8.7 and 1.5 g L^{-1} for PEG 600 and water, respectively), and a higher CO_2 concentration can enhance the current density for reduction. In order to examine the PEG effect on the improved performance of Au/C, two controlled Au catalysts were prepared: commercial Au/C (CM) and PEG-coated commercial Au/C (CM-PEG), which have the same particle size of approximately 25 nm. The total current density, CO production current, and Faradaic efficiency of CM-PEG and CM are displayed in Fig. 5b and d. The total current density for both CM-PEG and CM was 10 mA/cm^2 at −0.83 V, which is not changed by the presence of PEG. The overpotential at 10 mA/cm^2 of large CM-PEG and CM catalysts is approximately 300 mV larger than those for LS-PEG and LS. However, despite no difference in particle size, the enhanced CO production current and Faraday efficiency of CM-PEG compared with pristine CM was clearly observed, as shown in Fig. 5b and d. By simply coating a PEG layer on the commercial Au/C particles, CM-PEG presented an increased CO Faradaic efficiency with a maximum value of 75.6% at −0.77 V, whereas that of CM was 64%. In the potential ranges studied from −0.4 to −1.4 V, CM-PEG exhibited a higher CO Faradaic efficiency than the bare Au/C of CM. Overall, the control experiments revealed that PEG layers on the electrocatalyst effectively enhance the reaction selectivity for CO_2 reduction, and they provide a rationale for the improved performance of LS-PEG relative to LS.

However, the addition of PEG to Au/C does not change the potential where the peak CO Faradaic efficiency is found for LS-PEG and LS (i.e., −0.57 V) or for CM-PEG and CM (i.e., −0.77 V). In other words, both commercial and sputtered Au catalysts showed the same dependency of the CO Faradaic efficiency over the potentials shown in Fig. 5c and d, regardless of whether the PEG layer was present. Still, the CO selectivity and partial CO production rate did improve in the presence of the PEG layer. Thus, the role of the PEG layer appears to facilitate the CO_2 reduction reaction by creating a high CO_2 concentration region at the Au/C surface [38], but it does not actually affect the reaction kinetics. As discussed above, the improved performance of LS-PEG and CM-PEG over the LS and CM catalysts support the positive role of PEG in increasing the CO_2 concentration at the catalyst surface.

In addition, a few other possible effects of PEG on the increased CO Faradic efficiency at the Au/C surface were identified. Firstly, PEG may decompose during the electrochemical reactions. If PEG undergoes reduction or oxidation at the potential applied to Au/C, PEG acts as the reactant instead of CO_2 to produce CO or carbon-containing compounds such as $HCOO^-$, CH_3OH, C_2H_5OH, etc. However, the LSV results obtained with LS-PEG in an Ar-saturated 0.5 M $KHCO_3$ electrolyte without supplied CO_2 show that no hydrocarbons (including CO) were detected except for the formation of H_2 from proton reduction, thereby confirming that PEG did not decompose (Fig. S2). Further, if the PEG is consumed as a reactant, the CO production rate will decrease over a longer time in the CA experiments as the PEG decomposed. However, no degradation of LS-PEG was observed in the CA experiments after 10 h (Fig. 6, see below). Secondly, the performance of LS-PEG could be improved if electrical functionalization of its Au nanoparticles occurred as a result of PEG, in addition to the high CO_2 concentration by surface PEG molecules. However, the absorbance signal of the Au nanoparticles of LS-PEG in XAFS analysis matched that of Au foil exactly (Fig. S1a). Moreover, the Au signals of the prepared catalysts were not shifted in the XPS spectra (Fig. S1b), indicating there are no electrical interactions between the Au nanoparticles and the PEG layers. The physico-electrochemical analysis indicates that the PEG layers are not an oxidant and/or are electrically inert on the Au/C catalyst for CO_2 reduction. Consequently, this leads us to verify our assumption that the enhanced performance by the PEG layer is derived from certain physical properties of PEG (e.g., its high CO_2 solubility).

Additionally, the PEG layers are effective at maintaining the durability of Au/C in the CO_2 reduction reactions (Fig. 6). The catalytic stabilities of LS-PEG and LS were evaluated by CA at −0.77 V over 10 h

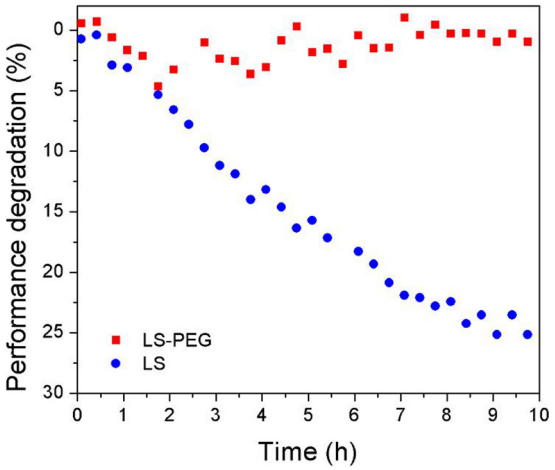

Fig. 6. Stability test of LS-PEG and LS catalyst over 10 h at −0.77 V.

in a CO_2-saturated 0.5 M $KHCO_3$ electrolyte. For longer times, the initial performance of LS-PEG maintained stability, while the performance of LS deteriorated by approximately 25%. To elucidate the reason of the enhanced stability, the surface state of the Au nanoparticles of LS-PEG and LS was analyzed using XPS after the CA. After the CA, an XPS-Au 4f peak at 85.5 eV, which is associated with binding between Au and S, emerged in LS after the stability test (Fig. 7); no distinctive change was observed for the Au 4f peak of LS-PEG after the CA. The appearance of Au-S bonding in LS implies that the performance degradation in CA is triggered by sulfur poisoning of the Au surfaces so as to inhibit active sites for CO_2 adsorption at Au. Sulfur bonded to Au in the LS electrode can be provided from the decomposition of sulfate from the Nafion binder added during electrode preparation. The decomposition of Nafion initiated by H- or OH- radical generation, and thereby yielding sulfide and free sulfate, has been suggested by Yu et al. [39]. When sulfide and sulfate are available at metal surfaces, sulfur-metal bonds can form via appropriate reduction reactions (Eqs. (1) and (2) [40]. The improved stability of LS-PEG without the formation of Au-S bonds indicates that the PEG layers protect the Au nanoparticles from sulfur poisoning in the presence of the Nafion binder in the electrochemical reduction of CO_2.

$$\text{Metal} + SO_3 + 6\,H^+ + 6\,e^- \rightarrow \text{Metal-S} + 3H_2O \quad (1)$$

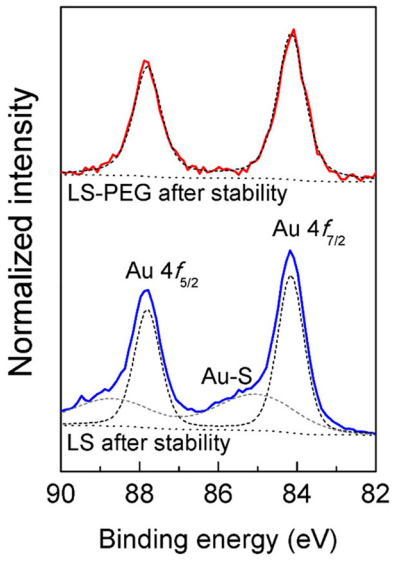

Fig. 7. XPS-Au4f analysis of LS-PEG (red) and LS (blue) after stability test.

Table 1
Performance comparison of previously reported Au nanoparticles.

Number	Reference	Size (nm)	Electrolyte	Max. CO F.E. (%)	CO F.E. at −0.6 V (vs. RHE)
1	This work	11	0.5 M $KHCO_3$	100	100
2	[36]	1	0.1 M $KHCO_3$	100	9.4
3	[36]	2	0.1 M $KHCO_3$	89	4.8
4	[36]	5	0.1 M $KHCO_3$	11	5
5	[37]	8	0.1 M $KHCO_3$	45	–
6	[41]	5	0.1 M $KHCO_3$	41	10
7	[42]	200	0.5 M $KHCO_3$	25	–
8	[43]	23	0.5 M $NaHCO_3$	99	–
9	[44]	8	0.5 M $KHCO_3$	97	93
10	[45]	7	0.1 M $KHCO_3$	83	83
11	[46]	3	0.5 M $NaHCO_3$	68	66

$$\text{Metal} + SO_4^{2-} + 8H^+ + 6e- \rightarrow \text{Metal-S} + 4H_2O \quad (2)$$

Finally, for objective performance comparison, previously reported Au nanoparticles and their CO_2 reduction performance are listed in Table 1 [36,37,41–46]. Au is one of the most notable CO_2 reduction catalysts for CO production; thus, a considerable number of Au-based catalysts have been developed. Since the early 1990 s, electrochemical CO_2 conversion began to be recognized as an eco-friendly and sustainable energy storage method. Among the selected performances of Au nanoparticles, LS-PEG demonstrates one of the most distinguishable CO_2 reduction activities at −0.57 V, with a CO Faradaic efficiency of 100%. Although further enhancements in activity must be sought to utilize Au nanoparticles for CO production in a practical manner, we believe that the PEG effect on CO_2 reduction activity and the simple synthetic method presented herein could provide tremendous insight to the industrialization of CO_2 conversion in terms of cost-effectiveness and eco-friendliness.

4. Conclusion

A PEG-coated Au/C catalyst was prepared via a liquid medium sputtering method with the use of PEG 600 as a liquid medium. This method enables a one-step synthesis of Au/C catalysts, which differs from chemical synthesis methods that typically require chemical reduction and ligand removal processes. The sputtering process employing PEG 600 induces coating of PEG layers on the Au/C catalyst, which enhances the performance of CO production. The prepared PEG-modified Au/C catalyst exhibited a Faradaic efficiency for CO production of 100% at −0.57 V. Based on the results of a PEG-removed Au/C catalyst and commercial Au/C catalysts, it was concluded that the high CO_2 solubility of PEG facilitates the CO_2 reduction reaction by creating a high CO_2 concentration region at the Au/C surface. Moreover, excellent catalytic durability is obtained by layering PEG on the Au/C electrodes because it prevents sulfur poisoning, that is, Au-S bond formation resulting from the decomposition of the Nafion binder during CO_2 reduction. Broadly, we anticipate the proposed catalytic activity and stability enhancement strategy, as well as the unique synthesis method using PEG sputtering, can further develop the industrialization of the electrochemical CO_2 conversion technique.

Acknowledgement

This study was supported by the Korean Government through the Korea CCS R&D Center (KCRC) grant funded by MSIT (No. 2014M1A8A1049349). This study was also financially supported by the KIST through the Institutional Project.

Appendix A. Supplementary data

Supplementary material related to this article can be found, in the online version, at doi:https://doi.org/10.1016/j.apcatb.2018.06.022.

References

[1] D.T. Whipple, P.J.A. Kenis, Prospects of CO2 utilization via direct heterogeneous electrochemical reduction, J. Phys. Chem. Lett. 1 (2010) 3451–3458.
[2] I. Zamboni, C. Courson, D. Niznansky, A. Kiennemann, Simultaneous catalytic H_2 production and CO_2 capture in steam reforming of toluene as tar model compound from biomass gasification, Appl. Catal. B: Environ. 145 (2014) 63–72.
[3] V.M. Lebarbier, R.A. Dagle, L. Kovarik, K.O. Albrecht, X.H. Li, L.Y. Li, C.E. Taylor, X. Bao, Y. Wang, Sorption-enhanced synthetic natural gas (SNG) production from syngas: a novel process combining CO methanation, water-gas shift, and CO_2 capture, Appl. Catal. B: Environ. 144 (2014) 223–232.
[4] C. Graves, S.D. Ebbesen, M. Mogensen, K.S. Lackner, Sustainable hydrocarbon fuels by recycling CO_2 and H_2O with renewable or nuclear energy, Renew. Sust. Energ. Rev. 15 (2011) 1–23.
[5] J.-P. Jones, G.K.S. Prakash, G.A. Olah, Electrochemical CO_2 reduction: recent advances and current trends, Isr. J. Chem. 54 (2014) 1451–1466.
[6] D.H. Won, H. Shin, J. Koh, J. Chung, H.S. Lee, H. Kim, S.I. Woo, Highly efficient, selective, and stable CO_2 electroreduction on a hexagonal Zn catalyst, Angew. Chem. Int. Ed. 55 (2016) 9297–9300.
[7] Z. Weng, J. Jing, Y. Wu, Z. Wu, X. Guo, K.L. Materna, W. Liu, V.S. Batista, G.W. Brudvig, H. Wang, Electrochemical CO_2 reduction to hydrocarbons on a heterogeneous molecular Cu catalyst in aqueous solution, J. Am. Chem. Soc. 138 (2016) 8076–8079.
[8] R. Kanega, N. Onishi, D.J. Szalda, M.Z. Ertem, J.T. Muckerman, E. Fujita, Y. Himeda, CO_2 hydrogenation catalysts with deprotonated picolinamide ligands, ACS Catal. 7 (2017) 6426–6429.
[9] A. Loiudice, P. Lobaccaro, E.A. Kamali, T. Thao, B.H. Huang, J.W. Ager, R. Buonsanti, Tailoring copper nanocrystals towards C_2 products in electrochemical CO_2 reduction, Angew. Chem. Int. Ed. 55 (2016) 5789–5792.
[10] J.H. Koh, D.H. Won, T. Eom, N.-K. Kim, K.D. Jung, H. Kim, Y.J. Hwang, B.K. Min, Facile CO_2 electro-reduction to formate via oxygen bidentate intermediate stabilized by high-index planes of Bi dendrite catalyst, ACS Catal. 7 (2017) 5071–5077.
[11] D.H. Won, C.H. Choi, J. Chung, M.W. Chung, E.-H. Kim, S.I. Woo, Rational design of a hierarchical Tin dendrite electrode for efficient electrochemical reduction of CO_2, ChemSusChem 8 (2015) 3092–3098.
[12] K.P. Kuhl, T. Hatsukade, E.R. Cave, D.N. Abram, J. Kibsgaard, T.F. Jaramillo, Electrocatalytic conversion of carbon dioxide to methane and methanol on transition metal surfaces, J. Am. Chem. Soc. 136 (2014) 14107–14113.
[13] K.-S. Kim, W.J. Kim, H.-K. Lim, E.K. Lee, H. Kim, Tuned chemical bonding ability of Au at grain boundaries for enhanced electrochemical CO_2 reduction, ACS Catal. 6 (2016) 4443–4448.
[14] J.-H. Kim, H. Woo, S.-W. Yun, H.-W. Jung, S. Back, Y. Jung, Y.-T. Kim, Highly active and selective Au thin layer on Cu polycrystalline surface prepared by galvanic displacement for the electrochemical reduction of CO_2 to CO, Appl. Catal. B: Environ. 213 (2017) 211–215.
[15] A. Januszewska, R. Jurczakowski, P.J. Kulesza, CO_2 electroreduction at bare and Cu-decorated Pd pseudomorphic layers: catalyst tuning by controlled and indirect supporting onto Au(111), Langmuir 30 (2014) 14314–14321.
[16] W. Zhu, Y.-J. Zhang, H. Zhang, H. Lv, Q. Li, R. Michalsky, A.A. Peterson, S. Sun, Active and selective conversion of CO_2 to CO on ultrathin Au nanowires, J. Am. Chem. Soc. 136 (2014) 16132–16135.
[17] S. Back, M.S. Yeom, Y. Jung, Active sites of Au and Ag nanoparticle catalysts for CO_2 electroreduction to CO, ACS Catal. 5 (2015) 5089–5096.
[18] H.-E. Lee, K.D. Yang, S.M. Yoon, H.-Y. Ahn, Y.Y. Lee, H. Chang, D.H. Jeong, Y.-S. Lee, M.Y. Kim, K.T. Nam, Concave rhombic dodecahedral Au nanocatalyst with multiple high-index facets for CO_2 reduction, ACS Nano 9 (2015) 8384–8393.
[19] J. Choi, M.J. Kim, S.H. Ahn, I. Choi, J.H. Jang, Y.S. Ham, J.J. Kim, S.-K. Kim, Electrochemical CO_2 reduction to CO on dendritic Ag-Cu electrocatalysts prepared by electrodeposition, Chem. Eng. J. 299 (2016) 37–44.
[20] D. Konig, K. Richter, A. Siegel, A.-V. Mudring, A. Ludwig, High-throughput fabrication of Au–Cu nanoparticle libraries by combinatorial sputtering in ionic liquids, Adv. Funct. Mater. 24 (2014) 2049–2056.
[21] D. Li, C. Wang, D. Tripkovic, S. Sun, N.M. Markovic, V.R. Stamenkovic, Surfactant removal for colloidal nanoparticles from solution synthesis: the effect on catalytic performance, ACS Catal. 2 (2012) 1358–1362.
[22] M.S. Wilson, S. Gottesfeld, Thin-film catalyst layers for polymer electrolyte fuel cell electrodes, J. Appl. Electrochem. 22 (1992) 1–7.
[23] I.Y. Cha, M. Ahn, S.J. Yoo, Y.-E. Sung, Facile synthesis of carbon supported metal nanoparticles via sputtering onto a liquid substrate and their electrochemical application, RSC Adv. 4 (2014) 38575–38580.
[24] T. Torimoto, K. Okazaki, T. Kiyama, K. Hirahara, N. Tanaka, S. Kuwabata, Sputter deposition onto ionic liquids: simple and clean synthesis of highly dispersed ultrafine metal nanoparticles, Appl. Phys. Lett. 89 (2006) 243117.
[25] Y. Hatakeyama, K. Asakura, S. Takahashi, K. Judai, K. Nishikawa, Microscopic structure of naked Au nanoparticles synthesized in typical ionic liquids by sputter deposition, J. Phys. Chem. C 118 (2014) 27973–27980.
[26] Y. Hatakeyama, K. Onishi, K. Nishikawa, Effects of sputtering conditions on formation of gold nanoparticles in sputter deposition technique, RSC Adv. 1 (2011) 1815–1821.

[27] E. Vanecht, K. Binnemans, J.W. Seo, L. Stappers, J. Fransaer, Growth of sputter-deposited gold nanoparticles in ionic liquids, Phys. Chem. Chem. Phys. 13 (2011) 13565–13571.
[28] S. Suzuki, T. Suzuki, Y. Tomita, M. Hirano, K. Okazaki, S. Kuwabata, T. Torimoto, Compositional control of AuPt nanoparticles synthesized in ionic liquids by the sputter deposition technique, CrystEngComm 14 (2012) 4922–4926.
[29] K. Okazaki, T. Kiyama, K. Hirahara, N. Tanaka, S. Kuwabata, T. Torimoto, Single-step synthesis of gold–silver alloy nanoparticles in ionic liquids by a sputter deposition technique, Chem. Commun. (2008) 691–693.
[30] Y. Oda, K. Hirano, K. Yoshii, S. Kuwabata, T. Torimoto, M. Miura, Palladium nanoparticles in ionic liquid by sputter deposition as catalysts for Suzuki-Miyaura coupling in water, Chem. Lett. 39 (2010) 1069–1071.
[31] T. Suzuki, S. Suzuki, Y. Tomita, K. Okazaki, T. Shibayama, S. Kuwabata, T. Torimoto, Fabrication of transition metal oxide nanoparticles highly dispersed in ionic liquids by sputter deposition, Chem. Lett. 39 (2010) 1072–1074.
[32] D. Koplijar, A. Inan, P. Vindayer, N. Wagner, E. Klemm, Electrochemcial reduction of CO2 to formate at high current density using gas diffusion electrodes, J. Appl. Electrochem. 44 (2014) 1107–1116.
[33] A.J. Bard, L.R. Faulkner, Electrochemical Methods: Fundamentals and Applications, 2nd ed., Wiley, New York, 2000.
[34] O. Aschenbrenner, P. Styring, Comparative study of solvent properties for carbon dioxide absorption, Energ. Environ. Sci. 3 (2010) 1106–1113.
[35] P. Lv, Z. Dong, X. Dai, Y. Zhao, X. Qiu, Low-dielectric polyimide nanofoams derived from 4,4'-(hexafluoroisopropylidene)diphthalic anhydride and 2,2'-bis(trifluoromethyl)benzidine, RSC Adv. 7 (2017) 4848–4854.
[36] D.R. Kauffman, D. Alfonso, C. Matranga, H. Qian, R. Jin, Experimental and computational investigation of Au_{25} clusters and CO_2: a unique interaction and enhanced electrocatalytic activity, J. Am. Chem. Soc. 134 (2012) 10237–10243.
[37] H. Mistry, R. Reske, Z. Zeng, Z.-J. Zhao, J. Greeley, P. Strasser, B.R. Cuenya, Exceptional size-dependent activity enhancement in the electroreduction of CO_2 over Au nanoparticles, J. Am. Chem. Soc. 136 (2014) 16473–16476.
[38] Z.Z. Yang, Q.W. Song, L.N. He, Capture and Utilization of Carbon Dioxide with Polyethylene Glycol, Springer, Berlin, 2012.
[39] T.H. Yu, W.-G. Liu, B.V. Merinov, P. Shirvanian, W.A. Goddard, III, mechanism for degradation of Nafion in PEM fuel cells from quantum mechanics calculations, J. Am. Chem. Soc. 133 (2011) 19857–19863.
[40] V.A. Sethuraman, J.W. Weidner, Analysis of sulfur poisoning on a PEM fuel cell electrode, Electrochim. Acta 55 (2010) 5683–5694.
[41] E. Andrews, S. Katla, C. Kumar, M. Patterson, P. Sprunger, J. Flake, Electrocatalytic reduction of CO_2 at Au nanoparticle electrodes: effects of interfacial chemistry on reduction behavior, J. Electrochem. Soc. 162 (2015) F1373–F1378.
[42] M. Liu, Y. Pang, B. Zhang, P. De Luna, O. Voznyy, J. Xu, X. Zheng, C.T. Dinh, F. Fan, C. Cao, F.P.G. de Arquer, T.S. Safaei, A. Mepham, A. Klinkova, E. Kumacheva, T. Filleter, D. Sinton, S.O. Kelley, E.H. Sargent, Enhanced electrocatalytic CO_2 reduction via field-induced reagent concentration, Nature 537 (2016) 382–386.
[43] Y. Chen, C.W. Li, M.W. Kanan, Aqueous CO_2 reduction at very low overpotential on oxide-derived Au nanoparticles, J. Am. Chem. Soc. 134 (2012) 19969–19972.
[44] W. Zhu, R. Michalsky, O. Metin, H. Lv, S. Guo, C.J. Wright, X. Sun, A.A. Peterson, S. Sun, Monodisperse Au nanoparticles for selective electrocatalytic reduction of CO_2 to CO, J. Am. Chem. Soc. 135 (2013) 16833–16836.
[45] Z. Cao, D. Kim, D. Hong, Y. Yu, J. Xu, S. Lin, X. Wen, E.M. Nichols, K. Jeong, J.A. Reimer, P.D. Yang, C.J. Chang, A molecular surface functionalization approach to tuning nanoparticle electrocatalysts for carbon dioxide reduction, J. Am. Chem. Soc. 138 (2016) 8120–8125.
[46] T.N. Huan, P. Prakash, P. Simon, G. Rousse, X. Xu, V. Artero, E. Gravel, E. Doris, M. Fontecave, CO_2 reduction to CO in water: carbon nanotube–gold nanohybrid as a selective and efficient electrocatalyst, ChemSusChem 9 (2016) 2317–2320.